On the origin of recent intraplate volcanism in Australia

D. Rhodri Davies[1] and Nicholas Rawlinson[2]
[1]Research School of Earth Sciences, The Australian National University, Canberra, ACT 0200, Australia
[2]School of Geosciences, University of Aberdeen, Aberdeen AB24 3UE, Scotland, UK

ABSTRACT

Many intraplate volcanic provinces do not appear to originate from plate-boundary processes or upwelling mantle plumes. Edge-driven convection (EDC), where a small-scale convective instability (induced by local variations in lithospheric thickness) displaces hot mantle material upward, provides an alternative hypothesis for such volcanism. Recently, EDC has been postulated as the trigger for Quaternary intraplate volcanism in Australia, due to the proximity of a craton edge. However, the Precambrian shield region of the Australian continent has a boundary that is at least 10,000 km long, yet the Newer Volcanics Province (NVP) is contained within a 400 × 100 km region. This brings into question EDC as a causal mechanism, unless nucleation at a single location can be explained. Here, we use a combination of seismic tomography and geodynamic modeling to show, for the first time, that (1) the source of the NVP is restricted to the upper mantle, and (2) mantle upwelling triggered by EDC is localized and intensified beneath the NVP as a result of three-dimensional variations in lithospheric thickness and plate motion–induced shear flow. This study helps to solve the global puzzle of why step changes in lithospheric thickness, which occur along craton edges and at passive margins, produce volcanism only at isolated locations.

INTRODUCTION

The widespread occurrence of intraplate volcanism is difficult to explain using the primary features of plate tectonics, such as subduction at convergent boundaries or upwelling at rifted margins, which are responsible for most volcanism on Earth. Instead, other mechanisms are invoked, including upwelling mantle plumes, edge-driven convection (EDC), shear-driven upwelling (SDU) of asthenosphere, and slab tear (e.g., King and Anderson, 1995, 1998; Davies and Davies, 2009; Conrad et al., 2011). The relative importance of these mechanisms is open to debate, and likely varies from one geological setting to the next.

In the case of EDC, numerical models are typically two-dimensional (2-D) and involve a step change or sharp transition in depth to the base of the lithosphere (King and Anderson, 1995). The implicit assumption in such models is that the step has significant continuity perpendicular to the plane of the experiment, such that the 2-D model is essentially a cross section of what would otherwise be a cylindrical or "Swiss roll"–type circulation pattern, with a central axis parallel to the strike of the step. Such a scenario has been invoked to explain intraplate volcanism observed along the transition between thick cratonic lithosphere and thin oceanic lithosphere (King and Ritsema, 2000). However, there are many regions where significant changes in lithospheric thickness occur, yet only a relatively small proportion of these have produced volcanism (King, 2007).

The Newer Volcanics Province (NVP) of Australia (Fig. 1), which ranges in age from 4.5 Ma to younger than 5 ka (Wellman, 1974), has been identified, on the basis of its proximity to a cratonic root, as one of ~20 volcanic provinces worldwide with a tectonic setting favorable for EDC (King, 2007). It is characterized by the existence of >700 eruption points, spread over an area >19,000 km^2 (Boyce, 2013), although the basaltic plains are generally <60 m thick, implying a low total eruption volume (Johnson, 1989). The distribution of volcanic centers is east-west, roughly perpendicular to the direction of current plate motion, and there is no associated age progression (Wellman, 1974).

Evidence pointing to the source of the NVP has so far been limited, with both Sr isotopic analysis (Price et al., 1997) and Re-Os isotopic analysis (McBride et al., 2001) unable to distinguish between a shallow or a deep mantle volcanic source. Global body-wave finite-frequency seismic tomography is not well resolved in southeast Australia, but on the basis of P- and S-wave images, the existence of a plume originating from the mid-mantle, centered beneath a region ~300 km southeast of the NVP, has been proposed (Montelli et al., 2006). Demidjuk et al. (2007) used simple low-Rayleigh-number, iso-viscous, 2-D numerical experiments to demonstrate that EDC can generate upwelling along an inferred step change in lithospheric thickness to the north of the NVP, which is consistent with the predictions of earlier work (e.g., King and Anderson, 1995, 1998). In a recent study, Holt et al. (2013) used geochemical analyses and thermodynamic modeling to show that the South Australian

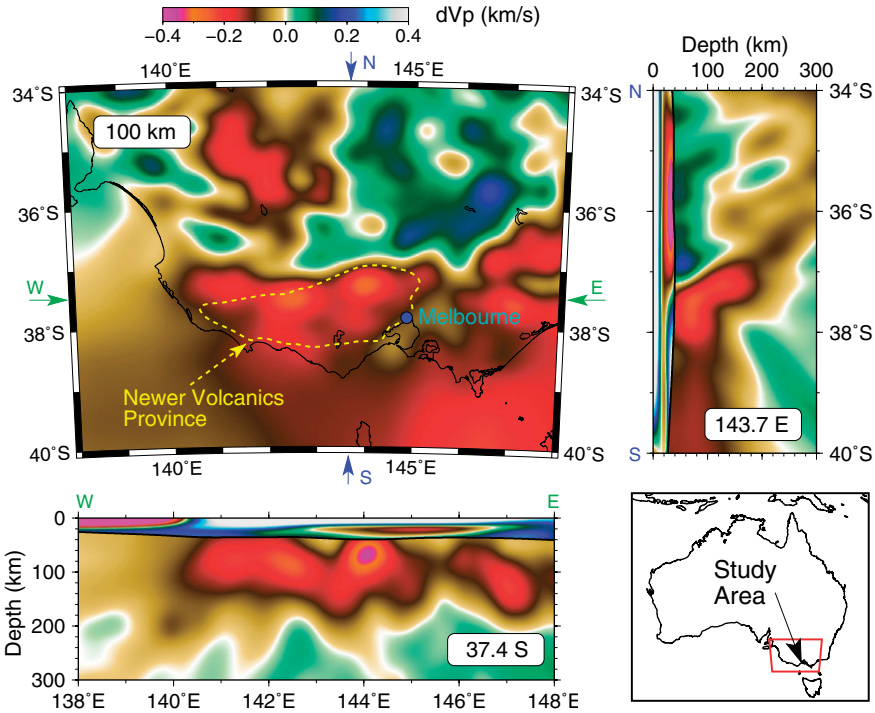

Figure 1. Variations in P-wave velocity for three orthogonal slices taken at 100 km depth (top left), 143.7°E (top right), and 37.4°S (bottom left) through the southeast Australian tomography model. Horizontal limits of Newer Volcanics Province (NVP) outcrop at the surface are denoted by yellow dashed line. Two vertical cross sections also reveal the presence of the *a priori* crustal layer.

component of the NVP was fed by magmas generated via decompressional melting, and that melt segregation occurred at pressures of 3–4 GPa, which correspond to the uppermost asthenosphere. While these analyses are consistent with the models of Demidjuk et al. (2007), no geodynamic scenario has been proposed to explain the localization of volcanism to a specific point along the southern cratonic boundary of Australia, despite recent 3-D modeling studies focusing on this region (Farrington et al., 2010) and similar tectonic settings elsewhere (e.g., Ramsay and Pysklywec, 2011). Instead, it has been proposed that compositional heterogeneities may provide a possible mechanism for more focused melting (Demidjuk et al., 2007).

3-D TELESEISMIC TOMOGRAPHY

We apply teleseismic tomography to a new seismic data set from the WOMBAT transportable array (operated by The Australian National University) in southeast Australia—the largest of its kind in the Southern Hemisphere—to image 3-D variations in upper mantle P-wave velocity beneath the NVP. Using a subset of distant earthquake recordings from 487 stations (see Fig. DR1 in the GSA Data Repository[1]), we invert relative arrival time residuals of global phases for variations in P-wave speed, using an iterative nonlinear technique (Rawlinson and Urvoy, 2006) (see the Data Repository for methods). Figure 1 shows a series of slices through the 3-D P-wave model, which reveals the presence of a low-velocity anomaly that spatially correlates with the surface expression of the NVP (see Figs. DR2–DR5 for reference model, ray path coverage, and resolution tests). The anomaly is clearly elongated in the east-west direction and extends to ~200 km depth, where it terminates. The peak of the anomaly, which is 0.4 km/s lower than the background velocity, occurs at ~144.0°E, 37.5°S, which corresponds, almost exactly, with the main concentration of volcanic centers at the surface (Boyce, 2013). Ostensibly, the new tomography results appear inconsistent with the presence of a mantle plume, which should correspond to a low-velocity zone extending into the deep mantle. One caveat, however, is that plumes may be narrower at greater depths, making them undetectable by tomography; another is that P-wave velocity becomes less sensitive to temperature with increasing depth. For instance, Cammarano et al. (2003) estimated that a temperature perturbation at 300 km depth produces less than 60% of the velocity change that would occur for the same perturbation at 100 km depth. However, the rapid decrease in velocity amplitude with depth that is imaged is far greater than the aforementioned estimate, making a plume scenario unlikely.

The low seismic velocities observed beneath the NVP may be due to the presence of elevated temperatures and/or partial melt, although with P-wave velocity alone, it is difficult to separate these contributions. If the anomaly is solely due to temperature, then the peak perturbation at 100 km depth would correspond to a temperature increase of ~500 °C (Cammarano et al., 2003), which is very large (plumes typically exhibit excess temperatures of 200–300 °C), notwithstanding uncertainties in the imaging results (see Figs. DR4 and DR5). At the other extreme, if the anomaly was solely due to the presence of partial melt, then the peak perturbation at 100 km depth would correspond to the presence of ~1% partial melt (Hammond and Humphreys, 2000). Exactly where along the trade-off curve between these two end members the anomaly beneath the NVP lies cannot be identified without further information, although the limited topographic response associated with the NVP would suggest that partial melt plays a significant role (Demidjuk et al., 2007).

GEODYNAMIC MODELS

Motivated by the seismic tomography results, which appear to support an upper mantle source for the NVP, we use geodynamic modeling to investigate whether EDC plays a central role in the origin of localized upwelling. To begin, we run a series of 2-D simulations to examine the relationship between the morphology and strength of EDC and two key geometrical parameters: (1) step height and (2) transition distance. We also examine the sensitivity of results to surface plate motions, thus accounting for potential contributions from SDU, which may be significant (Conrad et al., 2011). Our models solve for instantaneous mantle flow, where flow velocities and viscosities are determined in the presence of a prescribed temperature (density) field. Deformation is accommodated via a composite diffusion and dislocation creep, such that viscosity depends on temperature, pressure, and strain rate (see Table DR1 and the methods section of the Data Repository for justification of key parameter values). Calculations are undertaken using the recently developed Fluidity computational framework, which has been extensively benchmarked and validated for geodynamical simulation (e.g., Davies et al., 2011; Kramer et al., 2012).

The 2-D results (see the Data Repository and Figs. DR6 and DR7 therein) show that upwelling and downwelling velocities increase with step height, and that increasing the transition distance between thicker and thinner lithosphere displaces the convecting cell away from the base of the step. Increased plate velocities also displace the cell away from the step and result in an increase in upwelling velocity. We note that for all cases examined, peak velocities are significantly higher when accounting for the effects of dislocation creep. This important insight builds on those from previous 2-D numerical experiments (e.g., King and Anderson, 1998; Till and Elkins-Tanton, 2010; Farrington et al., 2010), which considered isoviscous or diffusion creep rheologies only.

To investigate the possible influence of 3-D effects that lie outside the plane of the experiment shown in Figure DR6, we construct a new map of the depth to the base of the lithosphere by combining constraints from a regional model and the new tomography results shown in Figure 1 (see the Data Repository). The new map (Fig. 2A) shows that the main "lithospheric step" is strongly modulated by variations in the third dimension. The NVP, which is located to the south of the step, lies at one end of a salient of thin lithosphere that extends northward toward the main step. For the purposes of regional 3-D geodynamic modeling, we distill this map into its key first-order features (Fig. 2B), which include several lithospheric steps in the neighborhood of the NVP. Our primary goal

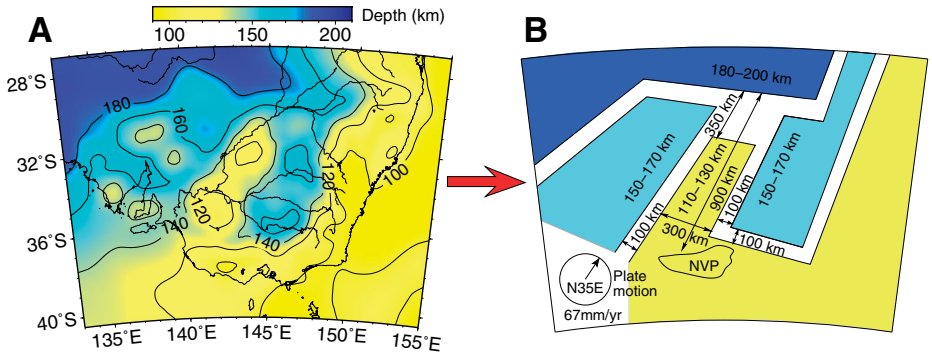

Figure 2. A: Estimate of depth to base of lithosphere using the seismic tomography results illustrated in Figure 1 combined with a regional model (see the Data Repository [see footnote 1]). B: Idealized version of A, constructed for input into three-dimensional geodynamic model. NVP—Newer Volcanics Province.

[1]GSA Data Repository item 2014358, methods for seismic tomography and geodynamic modelling, Table DR1, and Figures DR1–DR8, is available online at www.geosociety.org/pubs/ft2014.htm, or on request from editing@geosociety.org or Documents Secretary, GSA, P.O. Box 9140, Boulder, CO 80301, USA.

is to determine whether or not such complex 3-D lithospheric structure can explain the localization of volcanism to the NVP region; it is not to understand the temporal evolution of the NVP or surrounding lithosphere (although this is an important avenue for future research), therefore motivating the use of instantaneous flow models. In these models, we impose a 6.7 cm/yr N35E plate motion, which is approximately parallel to the northeast-trending salient of thinner lithosphere. Otherwise, all model parameters are identical to those of the 2-D experiments.

Figure 3 illustrates the regional 3-D modeling results, which predict maximum upwelling velocities of ~1.75 cm/yr (or ~1.10 cm/yr if dislocation creep is excluded). These large upwelling velocities are localized to a region that lies almost directly beneath the surface expression of the NVP and also dip toward the main lithospheric step, which is consistent with the tomographic observations of a northward-dipping low-velocity structure. When compared to a case that neglects surface plate motions (Fig. DR8a), (1) upwelling rates are slightly greater, which is consistent with the predictions from our 2-D models (Fig. DR7, right); (2) the edge-driven cell beneath the NVP is displaced away from the lithospheric step; and (3) the cell is isolated to the shallow asthenosphere (for the case with no plate motion, the cell extends to the base of the domain), which is consistent with the tomographic images.

To investigate how the orientation of a lithospheric step relative to the direction of plate motion influences upwelling rates, we ran a generic 3-D simulation in which an isolated lithospheric "keel," with a step height and transition distance that are identical to those of the main lithospheric step of our regional model, is used to induce EDC. The effects of SDU are subsequently superimposed, via the addition of 6.7 cm/yr plate motion (Fig. 4). In the absence of plate motion, EDC cells of equal strength are generated along all lithospheric steps, regardless of orientation. However, in the presence of plate motion, upwelling velocities are (1) enhanced on the lithospheric step where the mantle flows away from the craton, (2) reduced where the mantle flows toward the craton, and (3) marginally reduced on steps that are oriented parallel to the direction of plate motion. The most significant result of this test is that peak upwelling velocities, in the presence (absence) of plate motion, are ~1.15 (0.85) cm/yr, which is only ~65% (~50%) of that predicted beneath the NVP in our regional model (Fig. 3). This highlights the significant role played by 3-D lithospheric depth variations, which allow adjacent edge-driven cells to coalesce, thus enhancing and localizing mantle upwelling. Moreover, the interaction of EDC and plate motion–induced shear flow is important, not only for increasing upwelling velocities, but also for focusing flow toward the NVP, via the (lower pressure) narrow salient of thin lithosphere.

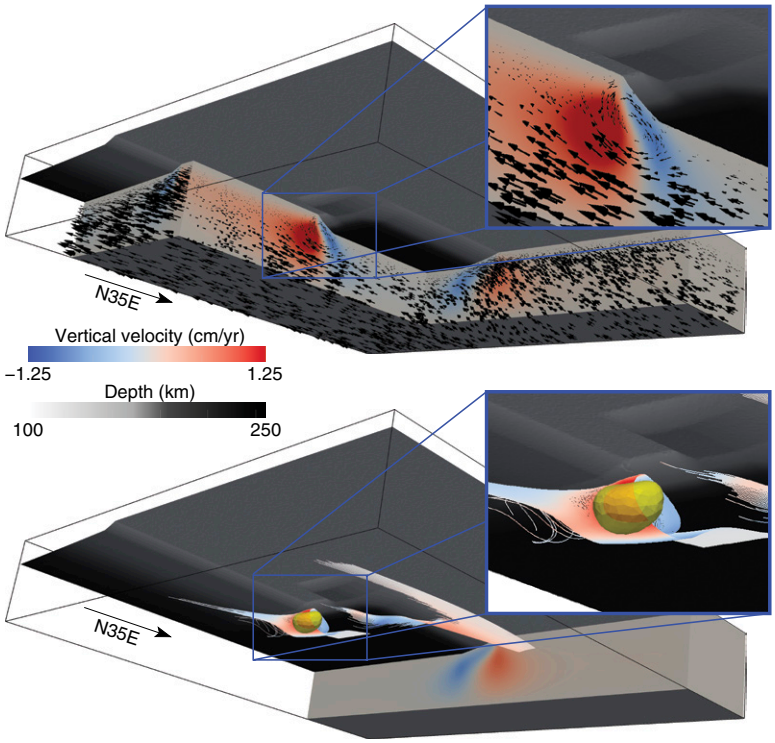

Figure 3. Mantle flow predicted by regional three-dimensional (3-D) geodynamic models in 3-D perspective, viewed from below. Computational domain is 700 km deep and 4200 km in all other directions. Images include (1) a temperature isosurface at 1400 K (grayscale), which approximates base of lithosphere and is colored by depth, with darker shades deeper than lighter shades; and (2) clipped surfaces, colored by vertical velocity, to illustrate the strength of edge-driven cells at various lithospheric steps. Upper image uses glyphs to represent velocity, thus providing insight into the flow pattern (note that the largest glyphs correspond to plate velocity of 6.7 cm/yr). These glyphs illustrate the recirculation cell that develops adjacent to the salient, with its axis aligned perpendicular to plate motion. In the bottom panel, stream tracers colored by vertical velocity are included (yellow isosurface outlines region where vertical velocities exceed 1.4 cm/yr) and clearly show that a cell forms only beneath the salient.

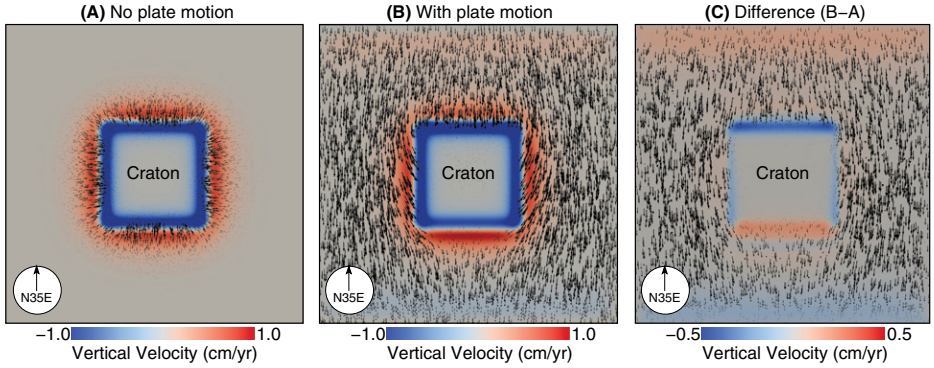

Figure 4. Interaction between edge-driven convection and shear-driven upwelling. Vertical velocity field (background fill) and glyphs at 200 km depth are from three-dimensional simulations, where an isolated craton is placed in the center of the computational domain (note that dimensions of the computational domain are identical to those shown in Figure 3, as are ages and transition distances of the craton and surrounding lithosphere). No plate motion is imposed for model shown in A, a plate velocity of 6.7 cm/yr is imposed in model shown in B, and the difference between these two models is illustrated in C. Maximum upwelling velocities are 0.85 cm/yr in A and 1.15 cm/yr in B.

The answer to the question of how mantle upwelling rates are related to melt production is not straightforward and depends on many factors (e.g., Raddick et al., 2002). For the upwelling rates associated with EDC, a prerequisite for melting is that the mantle must be close to its solidus, a condition that is met in our regional 3-D model, where temperatures within ~10

K of the wet (0.1 wt%) peridotite solidus are achieved at ~4 GPa (Katz et al., 2003). An estimate for melt production in an EDC-type scenario with an upwelling velocity of 1.5 cm/yr (comparable to our predictions for the NVP) places the rate of melt production (defined as the thickness of a horizontal layer formed by the accumulation of melt) at 2.5 km/m.y. (Conrad et al., 2010). However, the fraction of this amount that would erupt at the surface is unclear, so a direct comparison with NVP eruption volumes is not meaningful.

Variations in composition may also have a strong influence on melting: Demidjuk et al. (2007) showed that the NVP basalts with the largest ^{230}Th excesses contain enriched Sr-Nd isotope ratios, which they claim is evidence for substantial melting in the mantle. Convective entrainment of lithospheric material along the trailing edge of the cratonic keel, or inherited variability in the asthenosphere, are proposed as two possible sources of this enhanced fertility (Demidjuk et al., 2007). As noted previously, Holt et al. (2013) suggested that South Australian NVP basalts were produced by decompressional melting in the sublithospheric mantle. Their results imply upwelling rates of 1–2 cm/yr, which are consistent with those predicted beneath the NVP in our regional 3-D geodynamic model. Furthermore, the melt segregation pressures of 3–4 GPa calculated by Holt et al. (2013) coincide with our geotherm's closest approach to the peridotite solidus, providing further support to EDC, enhanced by plate motion–induced shear flow, as a causal mechanism.

CONCLUSIONS

This study is the first to document the behavior of EDC and SDU within a detailed 3-D framework, illustrating the importance of local variations in lithospheric thickness and plate motion in the localization of intraplate volcanism. A key outcome of this study is that it has yielded a geodynamic mechanism—consistent with detailed tomographic imaging—that explains shallow and localized upwelling beneath the NVP. Another important outcome is that although changes in lithospheric thickness are sufficient to trigger EDC, SDU is also vital for increasing upwelling rates, restricting circulation to the uppermost asthenosphere (see Fig. DR8) and displacing the edge-driven cell away from the lithospheric step (in this case, south toward the NVP). With this knowledge, the stage is set for future studies to investigate the temporal and spatial evolution of this system. Such studies may help to explain why the NVP is such a recent feature, and why southeast Australia has experienced intermittent low-volume intraplate volcanism for the past 190 m.y.

ACKNOWLEDGMENTS

We thank John Foden, Maxim Ballmer, and an anonymous reviewer for constructive comments on the original manuscript. Davies acknowledges Cian Wilson and Stephan Kramer for support with Fluidity. Numerical simulations were undertaken at the NCI National Facility in Canberra, Australia, which is supported by the Australian Commonwealth Government.

REFERENCES CITED

Boyce, J., 2013, The Newer Volcanics Province of southeastern Australia: A new classification scheme and distribution map for eruption centres: Australian Journal of Earth Sciences, v. 60, p. 449–462, doi:10.1080/08120099.2013.806954.

Cammarano, F., Goes, S., Vacher, P., and Giardini, D., 2003, Inferring upper-mantle temperatures from seismic velocities: Physics of the Earth and Planetary Interiors, v. 138, p. 197–222, doi:10.1016/S0031-9201(03)00156-0.

Conrad, C.P., Wu, B., Smith, E.I., Bianco, T.A., and Tibbetts, A., 2010, Shear-driven upwelling induced by lateral viscosity variations and asthenospheric shear: A mechanism for intraplate volcanism: Physics of the Earth and Planetary Interiors, v. 178, p. 162–175, doi:10.1016/j.pepi.2009.10.001.

Conrad, C.P., Bianco, T.A., Smith, E.I., and Wessel, P., 2011, Patterns of intra-plate volcanism controlled by asthenospheric shear: Nature Geoscience, v. 4, p. 317–321, doi:10.1038/ngeo1111.

Davies, D.R., and Davies, J.H., 2009, Thermally-driven mantle plumes reconcile multiple hotspot observations: Earth and Planetary Science Letters, v. 278, p. 50–54, doi:10.1016/j.epsl.2008.11.027.

Davies, D.R., Wilson, C.R., and Kramer, S.C., 2011, Fluidity: A fully unstructured anisotropic adaptive mesh computational modeling framework for geodynamics: Geochemistry Geophysics Geosystems, v. 12, Q06001, doi:10.1029/2011GC003551.

Demidjuk, Z., Turner, S., Sandiford, M., Rhiannon, G., Foden, J., and Etheridge, M., 2007, U-series isotope and geodynamic constraints on mantle melting processes beneath the Newer Volcanic Province in South Australia: Earth and Planetary Science Letters, v. 261, p. 517–533, doi:10.1016/j.epsl.2007.07.006.

Farrington, R.J., Stegman, D.R., Moresi, L.N., Sandiford, M., and May, D.A., 2010, Interactions of 3D mantle flow and continental lithosphere near passive margins: Tectonophysics, v. 483, p. 20–28, doi:10.1016/j.tecto.2009.10.008.

Hammond, W.C., and Humphreys, E.D., 2000, Upper mantle seismic wave velocity: Effects of realistic partial melt geometries: Journal of Geophysical Research, v. 105, p. 10,975–10,986, doi:10.1029/2000JB900041.

Holt, S.J., Holford, S.P., and Foden, J., 2013, New insights into the magmatic plumbing system of the South Australian Quaternary Basalt province from 3D seismic and geochemical data: Australian Journal of Earth Sciences, v. 60, p. 797–817, doi:10.1080/08120099.2013.865143.

Johnson, R.W., 1989, Intra-Plate Volcanism in Eastern Australia and New Zealand: New York, Cambridge University Press, 444 p.

Katz, R.F., Spiegelman, M., and Langmuir, C.H., 2003, A new parameterization of mantle melting: Geochemistry Geophysics Geosystems, v. 4, 1073, doi:10.1029/2002GC000433.

King, S.D., 2007, Hotspots and edge-driven convection: Geology, v. 35, p. 223–226, doi:10.1130/G23291A.1.

King, S.D., and Anderson, D.L., 1995, An alternative mechanism of flood basalt formation: Earth and Planetary Science Letters, v. 136, p. 269–279, doi:10.1016/0012-821X(95)00205-Q.

King, S.D., and Anderson, D.L., 1998, Edge-driven convection: Earth and Planetary Science Letters, v. 160, p. 289–296, doi:10.1016/S0012-821X(98)00089-2.

King, S.D., and Ritsema, J., 2000, African hotspot volcanism: Small-scale convection in the upper mantle beneath cratons: Science, v. 290, p. 1137–1140, doi:10.1126/science.290.5494.1137.

Kramer, S.C., Wilson, C.R., and Davies, D.R., 2012, An implicit free-surface algorithm for geodynamical simulations: Physics of the Earth and Planetary Interiors, v. 194–195, p. 25–37, doi:10.1016/j.pepi.2012.01.001.

McBride, J.S., Lambert, D.D., Nicholls, I.A., and Price, R.C., 2001, Osmium isotopic evidence for crust-mantle interaction in the genesis of continental intra-plate basalts from the Newer Volcanics Province, southeastern Australia: Journal of Petrology, v. 42, p. 1197–1218, doi:10.1093/petrology/42.6.1197.

Montelli, R., Nolet, G., Dahlen, F.A., and Masters, G., 2006, A catalogue of deep mantle plumes: New results from finite-frequency tomography: Geochemistry Geophysics Geosystems, v. 7, Q11007, doi:10.1029/2006GC001248.

Price, R.C., Gray, C.M., and Frey, F.A., 1997, Strontium isotopic and trace element heterogeneity in the plains basalts of the Newer Volcanic Province, Victoria, Australia: Geochimica et Cosmochimica Acta, v. 61, p. 171–192, doi:10.1016/S0016-7037(96)00318-3.

Raddick, M.J., Parmentier, E.M., and Scheirer, D.S., 2002, Buoyant decompression melting: A possible mechanism for intra-plate melting: Journal of Geophysical Research, v. 107, 2228, doi:10.1029/2001JB000617.

Ramsay, T., and Pysklywec, R., 2011, Anomalous bathymetry, 3D edge driven convection, and dynamic topography at the western Atlantic passive margin: Journal of Geodynamics, v. 52, p. 45–56, doi:10.1016/j.jog.2010.11.008.

Rawlinson, N., and Urvoy, M., 2006, Simultaneous inversion of active and passive source datasets for 3D seismic structure with application to Tasmania: Geophysical Research Letters, v. 33, L24313, doi:10.1029/2006GL028105.

Till, C.B., and Elkins-Tanton, L.T., 2010, A mechanism for low-extent melts at the lithosphere-asthenosphere boundary: Geochemistry Geophysics Geosystems, v. 11, Q10015, doi:10.1029/2010GC003234.

Wellman, P., 1974, Potassium-argon ages of the Cainozoic volcanic rocks of eastern Australia: Journal of the Geological Society of Australia, v. 21, p. 359–376, doi:10.1080/00167617408728858.

Manuscript received 17 July 2014
Revised manuscript received 2 September 2014
Manuscript accepted 3 September 2014

Printed in USA